Solar Phys (2009) 257: 83–90
DOI 10.1007/s11207-009-9334-9

Variability of Extended Bipolar Regions

W.B. Song · X.S. Feng · F. Shen · Y.Z. Zhang

Received: 30 December 2008 / Accepted: 13 March 2009 / Published online: 28 March 2009

Abstract Using NSO/Kitt Peak synoptic charts from 1975 to 2003, we group the main solar magnetic fields into two categories: one for active regions (ARs) and the other for extended bipolar regions (EBRs). Comparing them, we find that there exist three typical characteristics in the variability of EBRs: First, there exists a correlation between ARs and EBRs. The phase of EBR flux has a delay nearly two CRs. Second, we find that the EBR flux has two prominent periods at 1.79 years and 3.21 years. The 1.79-year period seems to only belong to large-scale magnetic features. Lastly, the North – South asymmetry of EBR flux is not very significant on a time scale of one solar cycle. However, during solar maxima, its dominance is found to shift from one hemisphere to the other.

Keywords Magnetic fields · Photosphere

1. Introduction

NSO/Kitt Peak magnetic synoptic charts have been made continuously over the past 30 years. They provide us with an opportunity to study the global distribution of solar magnetic fields through nearly three solar cycles. Many authors (*e.g.*, Knaack and Stenflo, 2005; Song and Wang, 2006) have discussed the characteristics of the total photospheric magnetic flux. However, few have included the statistics of the variability of extended bipolar regions (EBRs), which is possibly due to the uncertain and multiform EBR boundaries. Zhou, Wang, and Zhang (2006) found that 36% of Earth-directed coronal mass ejections (CMEs) came from EBRs and 11% of Earth-directed CMEs came from the long filaments along EBR boundaries. Thus EBRs are one of the main sources of CMEs and have important significance for space-weather studies. In this paper, using NSO/Kitt Peak synoptic charts, we group the main solar magnetic fields into two categories: one for active regions (ARs) and the other for EBRs. In what follows, by comparing them, we investigate some typical characteristics of the variabilities of EBRs.

W.B. Song (✉) · X.S. Feng · F. Shen · Y.Z. Zhang
SIGMA Weather Group, State Key Laboratory for Space Weather, Center for Space Science and Applied Research, Chinese Academy of Sciences, Beijing 100190, China
e-mail: wbsong@spaceweather.ac.cn

2. Selection Criteria for Extended Bipolar Regions

We define the EBR flux in 342 NSO/Kitt Peak synoptic charts from Carrington rotation (CR) 1666 to 2007. Kitt Peak charts have a grid of 360 equal steps in longitude by 180 equal steps in sine latitude. The pixel value is $B_v = B_l / \cos\phi$, where B_l denotes the flux density in gauss of the line-of-sight component of magnetic fields observed near the central meridian and ϕ is the latitude. Figure 1(a) gives an example for CR1985. When selecting EBR flux, we first find the strong and concentrated flux component related to ARs. Rabin *et al.* (1991) chose a threshold of 25 G as the separation between the strong and weak flux components. As shown in Figure 1(b), all of the black and white pixels' values are greater than 25 G. It is obvious that many, very small points are also included. To remove these points, which in fact do not belong to ARs, we define a function $f(k)$, where k is the distance between two pixels (where the unit is the grid of the magnetic chart) and $f(k)$ is the mean flux density of pixels with a distance $d \leq k$ (including $d = 0$) away from any chosen pixel. That is, all pixels in Figure 1(b) have $f(0) \geq 25$ G, in Figure 1(c) they have $f(\{0, 1\}) \geq 25$ G, and in Figure 1(f) they have $f(\{0, 1, 2, 3, 4\}) \geq 25$ G. For every CR, we use the same conditions as in Figure 1(f) to get the AR flux (or type I flux). As shown in Figure 1(f), when $s = 4$, the total number of pixels used in calculating the mean flux density is 49. This ensures an acceptable size of ARs and excludes the small and diffused but strong magnetic regions as

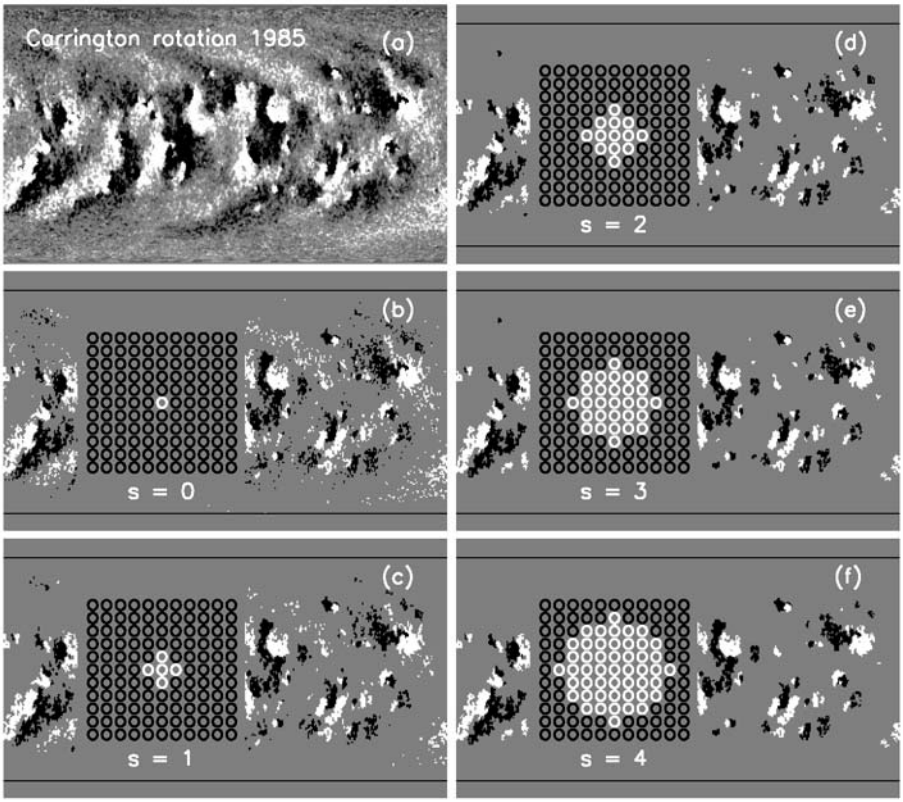

Figure 1 (a) NSO/Kitt Peak synoptic chart of Carrington rotation (CR) 1985. (b – f) For any $k \in \{0, 1, \ldots, s\}$, each pixel shown in the figure has $f(k) \geq 25$ G. When $s = 4$, all obtained pixels constitute type I flux.

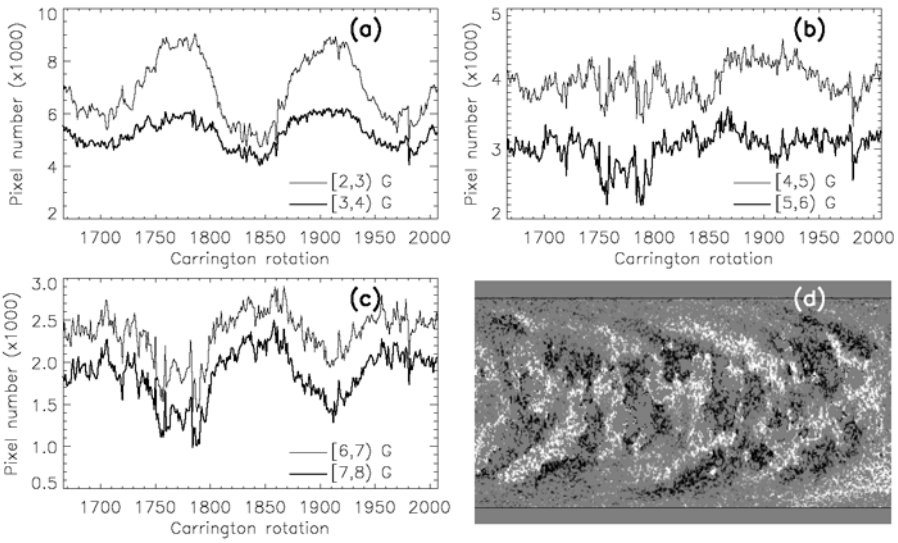

Figure 2 (a – c) Each CR's total number of pixels with values in $[2, 3), [3, 4), \ldots, [7, 8)$ G; (d) type II flux of CR1985.

well. EBRs often appear at the positions of ARs. Because the effect of differential rotation is rather strong at high latitudes, they are shaped like eyebrows. In Figures 2(a – c), we give the number of pixels with $B_v \in [n, n+1)$ G as a variation with CRs, where $n = 2, 3, \ldots, 7$. The 11-year solar cycle is abnormal until $n = 6$. Therefore we set two selection criteria for EBR flux (or type II flux): *i*) its pixel value $B_v \geq 6$ G and *ii*) the AR flux and polar regions ($\phi \geq 60^\circ$) are excluded. The EBR flux of CR1985 is shown in Figure 2(d).

3. Results and Discussion

The pixel area (a) of Kitt Peak charts is uniform and equals $4\pi {r_s}^2/(360 \times 180)$, where r_s is the solar radius. By adding $|B_v| \times a$ values of type I or type II pixels, we can obtain their respective total magnetic flux (TMF). As shown in Figures 3(a – b), the thin lines indicate the TMFs, and the thick lines denote the corresponding long-term variations derived from a simple Fourier filter ($f \leq \frac{6}{342}$ CR^{-1}). Figure 3(c) then gives the differences between the thin and thick lines, which indicate the short-term variations ($f \geq \frac{7}{342}$ CRs).

3.1. Flux Cross-Correlation

First, we study whether there exists a correlation between the two types of magnetic flux. To assess the degree of correlation, we compute the cross-correlation $[C(l)]$ as a function of the lag (l):

$$C(l) = \frac{\sum_{i=1}^{N-|l|} (x_{i+l_1} - \overline{x})(y_{i+l_2} - \overline{y})}{\sqrt{\sum_{i=1}^{N} (x_i - \overline{x})^2 \sum_{i=1}^{N} (y_i - \overline{y})^2}}, \tag{1}$$

where for $l < 0$, $[l_1, l_2] = [l, 0]$, and for $l \geq 0$, $[l_1, l_2] = [0, l]$. We use the F-test to estimate the significance level. The related function is $R_\alpha = \sqrt{\frac{F_\alpha(1,N-2)}{(N-2)+F_\alpha(1,N-2)}}$, where the value of

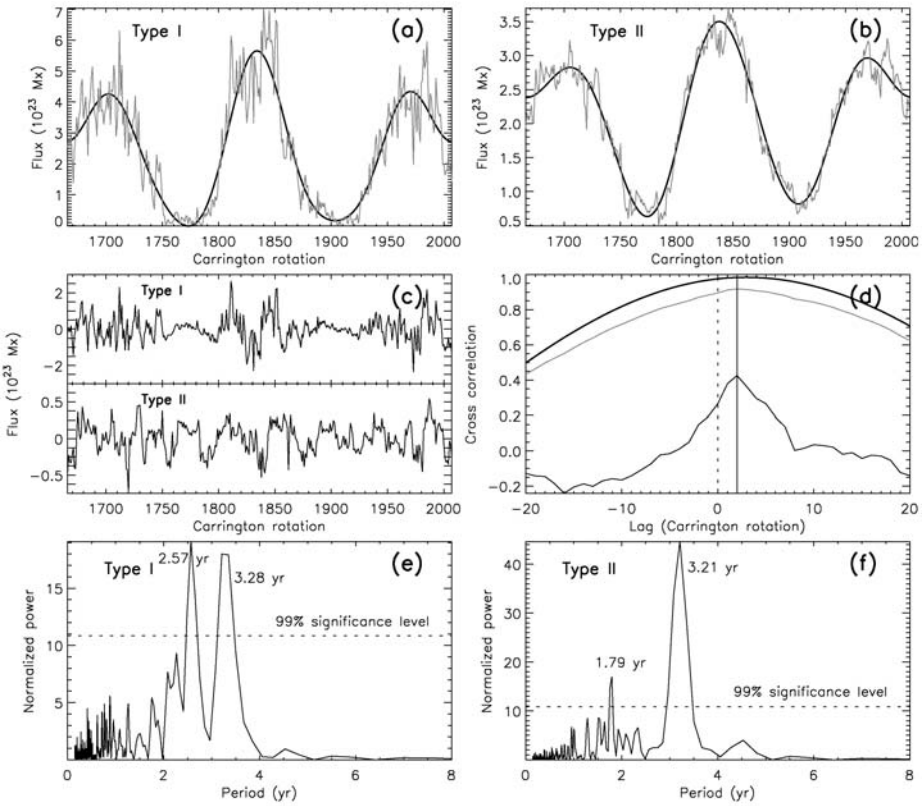

Figure 3 (a) and (b) The total magnetic flux (TMF) of type I and type II flux. Thick lines indicate the long-term variations derived from a Fourier filter. (c) Short-term variations, which equal the original TMFs subtracted from long-term variations. (d) Cross-correlations between the two types of magnetic flux (gray: original TMFs; thick: long-term variations; normal: short-term variations). (e) and (f) Scargle-normalized (divided by σ^2) periodograms of the short-term variations.

$F_\alpha(1, N-2)$ can be found in the F list at any given significance level (where $\alpha = 0.01$ and $N = 342$). Only if $C(l) \geq R_\alpha$ can we say that the correlation is significant.

For $l \in \{-20, -19, \ldots, 20\}$ we compute the $C(l)$ values of the long-term, short-term, and original TMFs, respectively. As shown by the solid vertical line in Figure 3(d), all sequences have a maximal $C(l) > R_\alpha = 0.14$ and they appear at a similar position of $l = 2$. This indicates that type I and type II flux have a significant correlation and a phase difference near two CRs. Generally speaking, EBRs come from the AR disruption under the combined effects of convective processes, large-scale flow, solar differential rotation, *etc*. Therefore the two-CR phase difference can be regarded as the average lifetime of ARs, which is much longer than the lifetime of most sunspots. At present, the lifetime of ARs has not received a great deal of attention possibly due to the difficulties in defining their terminations.

3.2. Periodicities

To search for the TMF periods of the two types of magnetic flux, we use the Scargle periodogram (Scargle, 1982). For a time sequence $x(t_i)$, including the uneven-sampling ones,

its Scargle power is defined to be

$$P(\omega) = \frac{1}{2}\left\{ \frac{[\sum_{i=1}^{N} x(t_i)\cos\omega(t_i-\tau)]^2}{\sum_{i=1}^{N}\cos^2\omega(t_i-\tau)} + \frac{[\sum_{i=1}^{N} x(t_i)\sin\omega(t_i-\tau)]^2}{\sum_{i=1}^{N}\sin^2\omega(t_i-\tau)} \right\}, \tag{2}$$

where $\tan 2\omega\tau = \sum_{i=1}^{N}\sin 2\omega t_i / \sum_{i=1}^{N}\cos 2\omega t_i$. Scargle's method has the advantage that for the independent and Gaussian-distributed noise with zero mean and constant variance (σ), the power density follows an exponential distribution. The probability of $P(\omega)$ at a given frequency being greater than K by chance equals e^{-K/σ^2}, so that Scargle's statistical significance level line is absolutely horizontal.

Figures 3(e – f) show the Scargle-normalized (divided by σ^2) power spectrum of the short-term variations of two TMFs. Above the 99% significance level lines we see two prominent peaks in type I flux, which are located at 2.57 and 3.28 years, and also two peaks in type II flux, which are located at 1.79 and 3.21 years. With regard to the common period, the 3.2-year period, Delache, Laclare, and Sadsaoud (1985) reported a similarly long one in the variability of the solar diameter. Özgüç, Ataç, and Rybák (2003) discovered that the flare indices during the past 40 years have a strong period of 3.1 years. Wolff (1992) suggested that a period of approximately three years might arise from the g modes beneath the envelope. Only type II flux has a 1.79-year period. Knaack, Stenflo, and Berdyugina (2004, 2005) found such a period in solar magnetic-flux asymmetry, especially at southern latitudes of 20° – 25°. Maravilla *et al.* (2001) found a persistent, prominent period at around 1.6 – 1.8 years in the time series of polar coronal hole areas from 1939 to 1996, covering five solar cycles. In the magnetic storm and sudden storm commencements at Earth, a spectral peak at 1.7 years was obtained by Mendoza *et al.* (1999). Meanwhile, such periods are not contained in type I flux. Thus we suggest that it should only belong to large-scale magnetic features, such as EBRs, coronal holes, *etc*. In contrast, another familiar period, the 155-day period, is found to be associated with those regions where magnetic fields are concentrated into small areas such as in sunspots, but not where they are more dispersed, as in plages (Lean and Brueckner, 1989).

3.3. North – South Asymmetries

In this section we discuss the TMF's North – South asymmetries (NSAs) of type I and type II magnetic flux. As usual, the NSA's degree is defined by

$$A_{NS} = \frac{N-S}{N+S}, \tag{3}$$

where N and S represent, respectively, the TMF values in northern and southern hemispheres. Figure 4 depicts all of the plots of N, S, and A_{NS} indices. Considering that both TMFs during solar minima (see the black vertical lines) are very small, we only study the NSA during other time intervals. To examine whether the NSA is a stochastic process, we introduce an estimation parameter based on the binomial distribution

$$P(n,d) = \sum_{k=d}^{n} \frac{n!}{k!(n-k)!} p^k (1-p)^{n-k}, \tag{4}$$

where n is the total number of samples and d is the number of occurrences of a certain event. If $P > 10\%$, the event can be believed not to have any statistical significance; if

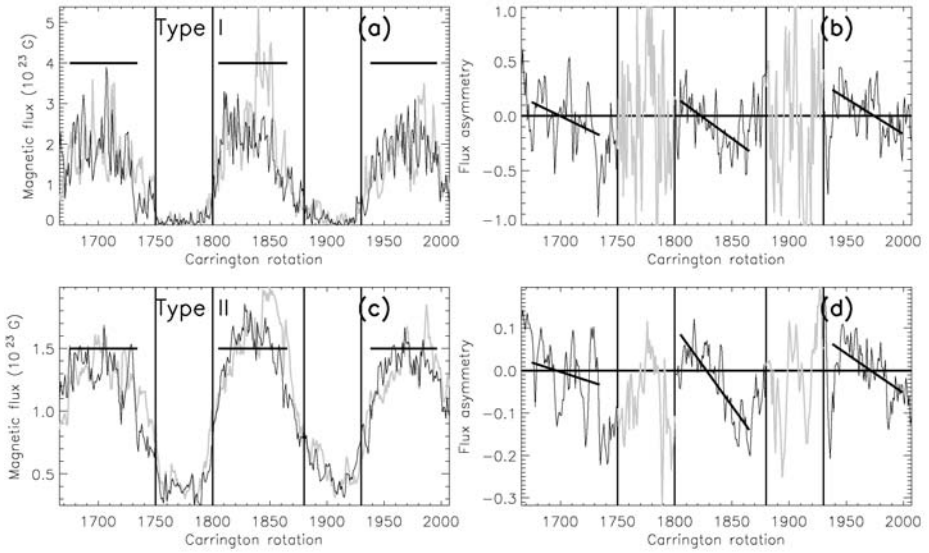

Figure 4 (a) and (c) TMF values of type I and type II magnetic flux in northern (black) and southern (gray) hemispheres; (b) and (d) North – South asymmetries. Black indicates solar maxima; gray indicates solar minima.

Table 1 North – South asymmetries (1: type I flux; 2: type II flux). n and s after d values mean the dominant hemisphere being the northern or the southern one. Time-1 indicates the interval of solar cycles excluding the minima. Time-2 indicates solar maxima. k is the slope of the black linear fitting curves in Figures 4(b) and (d).

Solar cycle	21	22	23
Time-1 (CR)	1666 – 1750	1800 – 1880	1930 – 2007
$(P, n, d)_1$	(6.42%, 85, 50s)	(5.96%, 81, 48s)	(36.72%, 78, 41n)
$(P, n, d)_2$	(50.00%, 85, 43n)	(3.74%, 81, 49s)	(45.50%, 78, 40s)
Time-2 (CR)	1675 – 1734	1805 – 1865	1938 – 1996
k_1 (CR^{-1})	-5.11×10^{-3}	-7.65×10^{-3}	-6.55×10^{-3}
k_2 (CR^{-1})	-0.88×10^{-3}	-3.74×10^{-3}	-1.86×10^{-3}

$1\% < P \leq 10\%$, we consider that some statistical significance exists, although it is not remarkable; if $P \leq 1\%$, an obvious statistical significance can be assumed (Carbonell, Oliver, and Ballester, 1993). For the NSA, White and Trotter (1977) pointed out that, as the average over a long time, the solar magnetic activity occurs in equal amounts in southern and northern hemispheres. Hence we can take $p = 0.5$. From Equation (3) we know that when $A_{NS} > 0$, the northern hemisphere is dominant, whereas when $A_{NS} < 0$, the southern hemisphere is dominant. Therefore, d can be chosen to be the number of samples in the dominant hemisphere. Table 1 lists P, n, and d values of two such types of magnetic flux during cycles 21 to 23. From this we find that there is no P value lying in the range of $\leq 1\%$. This suggests that the NSA is not remarkable on a time scale of a solar cycle (not including the minimum). Garcia (1990) came to a similar conclusion for the flare distribution.

From Figures 4(b) and (d) we observe an interesting trend that both fluxes dominate shifts from North to South during every solar maxima. Six black lines show the corresponding least-square linear fit of the NSA and as given in Table 1 their slopes (k) are all negative. Hansen and Hansen (1975) found that the dominance of solar filament activity shifted from the northern hemisphere to the southern hemisphere during the years 1964 to 1974 (cycle 20). Oliver and Ballester (1994) noticed the same phenomenon in sunspot area during the years 1983 to 1993 (cycle 22). Vizoso and Ballester (1990) analyzed the NSA of sunspot area during the years 1874 to 1976 and found that the activity in one hemisphere was more important during the ascending branch of the cycle while during the descending branch the activity became more important in the opposite hemisphere. To explain this regularity of dominance passing from North to South, we suppose that the time of reaching activity maximum is different for the two hemispheres. During cycles 21 to 23, the activity peak time of the northern hemisphere is always earlier than that of the southern one. At the beginning of the solar cycle, solar activity is dominant in the northern hemisphere. Then the activity level of the northern hemisphere starts to decline, but that of the southern one still gets stronger. Before long, the dominance will shift to the South. According to other NSA results (*e.g.*, Hansen and Hansen, 1975; Özgüç and Üçer, 1987) we do not think that the peak time of the northern hemisphere is always earlier than that of the southern one. Sometimes it is later than the southern one so that the dominance would shift from South to North. If they appear at the same time, the NSA would become unclear throughout the whole solar cycle.

4. Summary

In this investigation we divide the main solar magnetic fields into two categories: one for ARs and the other for EBRs. By making a comparison between them, we find three typical characteristics in the variability of EBRs: First, there exists a correlation between ARs and EBRs. The phase of EBR flux has a delay of nearly two CRs. Second, we find that the sequence of EBR TMF has two prominent periods at 1.79 and 3.21 years. The 1.79-year period possibly only belongs to large-scale magnetic features. Lastly, the NSA of EBR flux is not very significant on a time scale of one solar cycle. However, during solar maxima, its dominance is found to shift from one hemisphere to the other. In some sense, our selection criteria for EBRs is presently a bit arbitrary (for example, potentially including some ephemeral regions and excluding some poleward-migrating flux at high latitudes). It is hoped that substantial improvement or new criteria can be made for the selection of EBRs in the future.

Acknowledgements This work is jointly supported by the National Natural Science Foundation of China (40536029, 40604019, 40621003, and 40890160), the 973 project under Grant No. 2006CB806304, and the Specialized Research Fund for State Key Laboratories.

References

Carbonell, M., Oliver, R., Ballester, J.L.: 1993, *Astron. Astrophys.* **274**, 497.
Delache, P., Laclare, F., Sadsaoud, H.: 1985, *Nature* **317**, 416.
Garcia, H.A.: 1990, *Solar Phys.* **127**, 185.
Hansen, R., Hansen, S.: 1975, *Solar Phys.* **44**, 225.
Knaack, R., Stenflo, J.O.: 2005, *Astron. Astrophys.* **438**, 349.
Knaack, R., Stenflo, J.O., Berdyugina, S.V.: 2004, *Astron. Astrophys.* **418**, L17.
Knaack, R., Stenflo, J.O., Berdyugina, S.V.: 2005, *Astron. Astrophys.* **438**, 1067.

Lean, J.L., Brueckner, G.E.: 1989, *Astrophys. J.* **337**, 568.
Maravilla, D., Lara, A., Valdés-Galicia, J.F., Mendoza, B.: 2001, *Solar Phys.* **203**, 27.
Mendoza, B., Lara, A., Maravilla, D., Valdés-Galicia, J.F.: 1999, *Solar Phys.* **185**, 405.
Oliver, R., Ballester, J.L.: 1994, *Solar Phys.* **152**, 481.
Özgüç, A., Üçer, C.: 1987, *Solar Phys.* **114**, 141.
Özgüç, A., Ataç, T., Rybák, J.: 2003, *Solar Phys.* **214**, 375.
Rabin, D.M., DeVore, C.R., Sheeley, N.R., Harvey, K.L., Hoeksema, J.T.: 1991, In: Cox, A.C., Livingston, W.C., Matthews, M.S. (eds.) *Solar Interior and Atmosphere*, Univ. Arizona Press, Tucson, 781
Scargle, J.D.: 1982, *Astrophys. J.* **263**, 835.
Song, W.B., Wang, J.X.: 2006, *Astrophys. J.* **643**, L69.
Vizoso, G., Ballester, J.L.: 1990, *Astron. Astrophys.* **229**, 540.
White, O.R., Trotter, D.E.: 1977, *Astrophys. J. Suppl.* **33**, 391.
Wolff, C.L.: 1992, *Solar Phys.* **142**, 187.
Zhou, G.P., Wang, J.X., Zhang, J.: 2006, *Astron. Astrophys.* **445**, 1133.